I. J. Engineering and Manufacturing, **2022, 1, 37-47**
Published Online February 2022 in MECS (http://www.mecs-press.org/)
DOI: 10.5815/ijem.2022.01.04

Design of the Wing of a Medium Altitude Long Endurance UAV

Oluwafemi A. Adeleke[a,*], Godwin E. Abbe[a], Paul O. Jemitola[a], Sadiq Thomas[b]
[a]Department of Aerospace Engineering, Faculty of Air Engineering, Air Force Institute of Technology, Kaduna, Nigeria
[b]Department of Computer Engineering, Faculty of Engineering, Nile University of Nigeria, Abuja, Nigeria
E-mail: oluwafemianthony.adeleke@gmail.com

Received: 14 July 2021; Revised: 25 August 2021; Accepted: 28 October 2021; Published: 08 February 2022

Abstract: Over time, the need to extend the endurance of fixed-wing UAVs has been a challenge and requirement for the aviation industry. As a result, there are many ongoing researches on how to address this challenge while developing new concepts for an aircraft wing. This paper presents the methodology applied in the design of the wing of a lightweight unmanned aerial vehicle (UAV) that is intended for intelligence and surveillance (ISR) missions. A conceptual design was developed with the aircraft having a hybrid wing for the purpose of improving its structural design. The wing has two spars and thirteen ribs a side with an all-composite structure. Initial calculations were performed theoretically, thereafter, analyzed using the finite element analysis tool.

Index Terms: Wing Design, Unmanned Aerial Vehicle, Aircraft Structure

1. Introduction

Engineering design involves a process which is usually iterative in the form of a continual feedback of information to check the assumptions made at the initial stage [1]. The methods adopted in the design process of an aircraft usually involve the following activities [2]:

1. Problem solving through engineering or mathematical calculations; and
2. Choosing a preferred method among many alternatives.

Increase in demands in the rate of production and performance of aircraft has led to the research for newness in the design and manufacturing of aircraft wings with the use of UAVs being more pronounced these days. Therefore, it is pertinent to consider the characteristics, assembly and manufacturing method for the wing which are some of the key drivers for the design of next generation wings. The wing of a UAV according to its mission and/or intended role varies in airfoil shape, chord dimensions, span, surface area and geometry [3]. Fig 1 shows a typical example of an aircraft wing.

Aircraft are majorly classified by their wing configuration. The conceptual design of the wing adopted for this UAV is a “V-tail high wing cantilever monoplane of straight constant chord with tapered outer sections”. High wing aircraft are inherently stable as their center of mass is located below the center of lift and with high aspect ratio, they usually experience less induced drag and reduced fuel consumption [5].

However, to get a critical design objective, it was important to study similar UAVs in the same weight category. The design methodology adopted involves:

1. Calculating the design speeds and maneuver flight envelope.
2. Determining the critical loads which act on the aircraft and sizing the wing structure based on those loads.
3. Producing a CAD model.

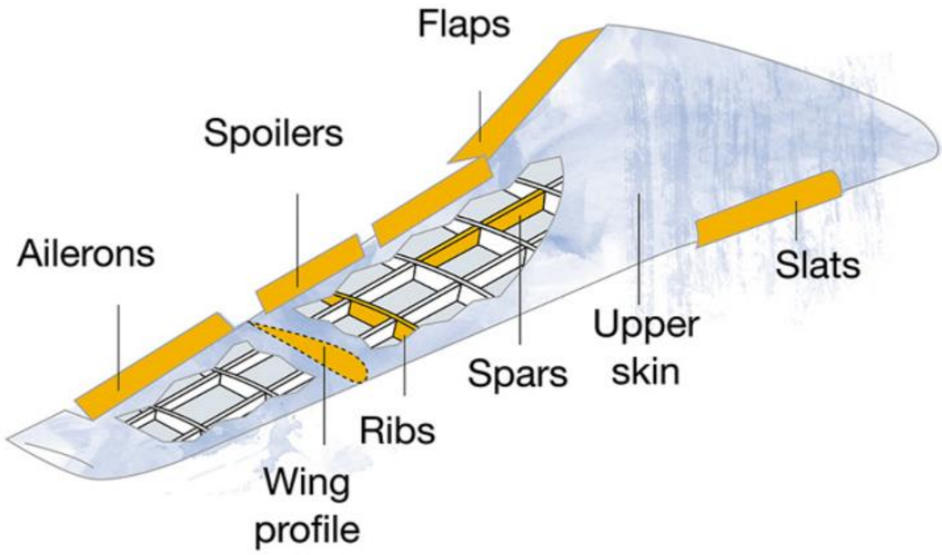

Fig. 1. Typical aircraft wing [4]

Nomenclature

a_{2A}	aileron lift curve slope
a_{1WB}	wing-body lift curve slope
ac	further nomenclature continues down the page inside the text box
b	wingspan
$\bar{c}$	standard or geometric mean chord (SMC)
c	mean aerodynamic chord (MAC)
cg	center of gravity
C_D	drag coefficient
C_L	lift coefficient
C_{Mo}	zero lift pitching moment coefficient
g	acceleration due to gravity
h	location of cg as a fraction of MAC
H_o	location of aerodynamic center as a fraction of MAC
I_x	mass moment of inertia in roll
k_x	roll radius of gyration
K_g	gust alleviation factor
l'_t	distance from aircraft cg to tail aerodynamic center
L_ξ	rolling moment due to aileron deflection
L_p	rolling moment due to roll rate
L_T	horizontal stabilizer or tail plane load
L_{WB}	wing-body load
L_{WO}	increment of wing load due to control deflection
m	maximum take-off weight
n	load factor
$\dot{p}$	maximum roll acceleration
S	wing area
T	thrust
U_{de}	derived gust velocity
V_A	design maneuvering speed
V_C	design cruise speed
V_D	design dive speed
V_F	design flap speed
V_{S1}	design stall speed
z_t	distance of thrust axis above cg

2. Literature Review

Aircraft design has evolved over the years from the first flight of the Wright brothers (Orville and Wilbur) in 1903. The design of the wing is very important for an aircraft as it directly affects the aerodynamic shape, drag, range, maximum speed, and maneuverability [2].

Naidu and Adali (2014) designed the wing of a lightweight Medium Altitude Long Endurance (MALE) Unmanned Aerial Vehicle (UAV) intended for intelligent and surveillance (ISR) missions. The aircraft was designed and optimized to incorporate a relatively high aspect ratio to decrease drag and extend the flight time. The wingbox was modelled using FEA for a maximum loading condition of +3.2g [8].

Grodzki and Lukaszewicz (2015) designed the wing of an unmanned aerial vehicle as a multistage task which included: airfoil selection, geometrical calculations, structural design, materials selection, numerical analysis, and elaboration of technolgy. The simulation was carried out in SolidWorks environment while creating variety of composite structures, analyzing them and comparing their strength properties to provide valuable information in the early design stage [3].

Yu (2018) compared several types of wing such as the beam-type, single-block type, and multi-ventral plate type and chose the beam-type wing. Thereafter, performed detailed design and optimization to reduce the weight of the wing. CATIA was employed to design the 3D model for a potential realistic production [18].

Chauhan *et. al* (2017) attempted to formulate the structural design process for a UAV wing and subsequent optimization for SAE India Aero Design Challenge 2017. The design commenced with the identification of the structural design parameters and challenge requirements. Based on the engineering values, a mathematical interface was coded in MATLAB to calculate the mechanical equivalents for the wing at individual sections. The structural design of the wing was modelled in SolidWorks with the final mass calculated in the Preliminary Design Phase. For initial estimates, the static structural analysis of the layout was performed theoretically. However, the final design of the wing was imported into ANSYS Finite Element solver for static structural analysis. Successive iterations were performed with the final simulation of the wing which gave a safety factor of 3.73 [19].

A comparative study was carried out on UAV designs with intended weight category of similar configuration and statistical data such as the Bayraktar Tactitical UAS, Elbit Systems Hermes 900 designed in accordance with (IAW) STANAG 4671, Thales Watchkeeper WK4450 and TAI Anka. The statistical data from the prototypes with empirical formulae for determining geometrical parameters as presented by Raymer and Gudmundsson [6,7] were used to derive the initial data of the proposed aircraft.

3. Design Analysis

Loads are applied to all major structural components of the aircraft. The structural load analysis helps in calculating the loads acting on the structure of the aircraft for flight maneuvers [9]. Therefore, there is a need to determine the wing loads for a proper structural design. To calculate the load actions analysis of the UAV, we must first establish its center of gravity location and subsequently determine the mass moments of inertia in roll, pitch, and yaw. The overall location of the cg was based on mass breakdown of each component and their respective cg locations taking the nose of the aircraft as the datum reference.

The n-V diagram was constructed for the most critical flight envelope which is the operating empty weight at mean sea level, see Fig 2. The diagram was produced in accordance with STANAG 4671 which has an airworthiness requirement for fixed wing UAV systems of maximum take-off weight of more than 150kg and less than 20,000kg [10]. Table 1 shows the fundamental data for the proposed aircraft as derived from initial sizing. The constraint analysis method was used to determine the appropriate wing area based on the intended aircraft role and mission.

Table 1. Fundamental aircraft data [11]

Parameter	Value
Maximum take-off weight, MTOW	650 kg
Operating empty weight, OEW	332.95 kg
Wing area, S	10.36 m^2
Mean aerodynamic chord, MAC	0.9 m
Cruise altitude	15,000 ft
Endurance	24 hrs

The positive and negative maneuvering load factors as specified by STANAG are 3.8 and -1.5 respectively. This was used in deriving the n-V diagrams and calculations. The requirements for the Equivalent Airspeeds (EAS) are calculated as follows:

Design cruising speed,

$$V_C = 2.4\sqrt{Mg/S} \tag{1}$$

Design dive speed,

$$V_D = 1.25V_C \tag{2}$$

Design stall speed,

$$V_{S1} = \sqrt{\frac{2W}{\rho C_{Lmax} S}} \tag{3}$$

where the maximum positive lift coefficient, C_{Lmax}, was derived as 1.416 and air density at sea level, ρ, is given from standard atmosphere table as 1.225kg/m^3.

Design maneuvering speed,

$$V_A = V_{S1}\sqrt{n} \tag{4}$$

STANAG prescribed that gust velocities of 15.2m/s at V_C must be considered at altitudes between sea level and 20,000ft, and 7.6m/s for altitudes from 20,000ft to 50,000ft while 7.6m/s at V_D must be considered at altitudes between sea level and 20,000ft, and 3.8m/s for altitudes from 20,000ft to 50,000ft [10]. However, the gust load factors were derived using the procedure outlined in CS-VLA which is an airworthiness code applicable to single-engine aircraft with a certified take-off weight of not more than 750kg.

Aircraft mass ratio,

$$\mu_g = \frac{2(m/S)}{\rho \bar{C} a_{1WB}} \tag{5}$$

where the wing-body lift curve slope and the geometric mean chord were gotten as 5.175/rad and 0.942m respectively.

Gust alleviation factor,

$$K_g = \frac{0.88\mu_g}{5.3+\mu_g} \tag{6}$$

Gust load factor,

$$n = 1 \pm \frac{1/2\rho_0 V a_{1WB} K_g U_{de}}{mg/S} \tag{7}$$

At V_C, maximum positive gust load factor n_3 = 4.84, and negative n_4 = -2.84. At V_D, maximum positive gust load factor n_3 = 3.40, and negative n_4 = -1.40.

The equivalent airspeeds at sea level, transition altitudes, cruise altitude and the service ceiling calculated theoretically using Equation (1-7) are detailed in Table 2.

Table 2. Design equivalent airspeed

		SL	7,500ft	15,000ft	22,000ft	30,000ft
OEW	V_{s1} (m/s)	19.06	19.06	19.06	19.06	19.06
	V_A (m/s)	37.16	37.16	37.16	37.16	37.16
	V_F (m/s)	26.69	26.69	26.69	26.69	26.69
	V_C (m/s)	42.61	38.07	33.80	30.05	26.06
	V_D (m/s)	53.26	47.58	42.24	37.57	32.58
MTOW	V_{s1} (m/s)	26.63	26.63	26.63	26.63	26.63
	V_A (m/s)	51.92	51.92	51.92	51.92	51.92
	V_F (m/s)	37.29	37.29	37.29	37.29	37.29
	V_C (m/s)	59.53	53.19	47.22	41.99	36.41
	V_D (m/s)	74.41	66.49	59.03	52.49	45.52

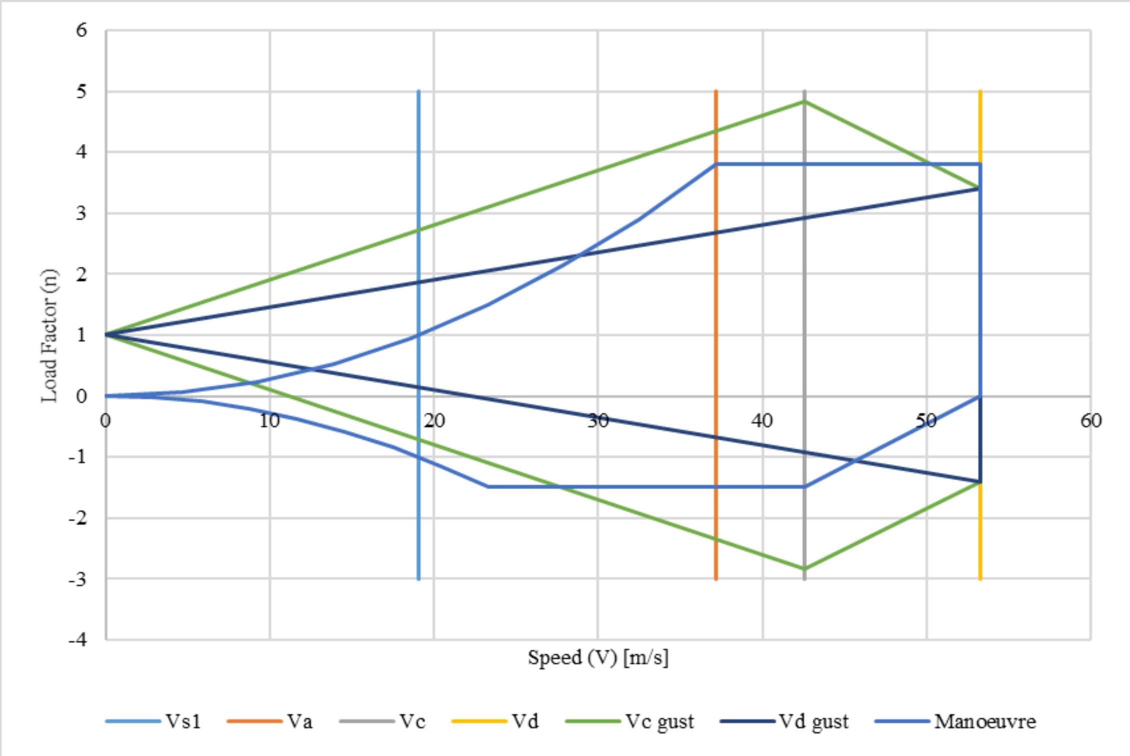

Fig. 2. Maneuvering and gust envelope at operating empty weight

3.1. Load action analysis

The loads that will act on the wing have to be calculated to enable proper sizing since the wing carries 95% of the total loads acting on the aircraft. As such, the failure of the wing structure will invariably lead to the failure of the whole aircraft. All the loads were calculated theoretically using known empirical formulae with the help of Microsoft excel spreadsheet. Each flight condition was analyzed with the aircraft in various configurations of altitude, velocity, mass, and load factor of the flight envelope. The largest wing-body load was obtained as 27,488N at a sudden maximum aileron deflection at V_A (maneuvering speed) for maximum take-off weight at sea level. The following equations from Denis Howe [12] were used to determine the tail load on the aircraft at symmetric loading except otherwise stated:

$$L_T = \left[M_o + ngm(h - H_o)c + Tz_t - K_y{}^2\ddot{\theta}\right]/l'_t \tag{8}$$

where the zero-lift pitching moment, M_o, is given by [13]:

$$M_o = 0.5\rho V^2 ScC_{Mo} \tag{9}$$

The moment created by the lift from the wing-body, M_{WB}, is given by:

$$M_{WB} = ngm(h - H_o)c \tag{10}$$

In this case, h = 0.188 for the forward CG position, H_o = 0.25 and load factor (n) for steady trimmed level flight = 1.

For steady level flight, it was assumed that thrust is equal to drag. Hence,

$$T = D = 0.5\rho V^2 SC_D \tag{11}$$

Lift Coefficient [13]

$$C_L = \frac{L}{0.5\rho V^2 S} = \frac{mg}{0.5\rho V^2 S} \tag{12}$$

where the thrust offset below the aircraft center of gravity, $z_t = 0.34$m

Moment due to thrust,

$$M_{Zt} = T * Z_t \tag{13}$$

Note: $K_y{}^2\ddot{\theta}$ was assumed to be negligible for a steady level flight since there is no angular acceleration. Distance from the aircraft CG to tail aerodynamic center, $l'_t = 1.842$m.

To achieve equilibrium of forces in a steady level flight

$$L_{WB} + L_T - ngm = 0 \tag{14}$$

The following method was used to calculate the aileron loads for case 1 (full deflection at VA):

Rolling moment due to roll [14],

$$L_p = C_{lp}(\rho V_o S b^2/4I_x) \tag{15}$$

where variation of roll moment coefficient with roll rate C_{lp} was gotten from AVL [17] as -0.5573, yaw moment of inertia $I_x = 17.41\text{kgm}^2$, and maneuvering speed $V_A = 51.921$m/s at sea level.

Rolling moment due to aileron deflection [14],

$$L_\xi = C_{l\delta}\left(\rho V_o{}^2 Sb/2I_x\right) \tag{16}$$

where variation of roll moment coefficient with aileron $C_{l\delta} = 0.0051$ from AVL

Maximum roll acceleration

$$(\dot{p})_{max} = (\rho V_o{}^2 SbL_\xi/2)(mk_x{}^2) \tag{17}$$

where the roll radius of gyration $k_x = 0.1637$

Maximum steady rate off roll,

$$(p)_{max} = -(V_o/b)(\,L_\xi/L_p)\xi \tag{18}$$

The value used for the aileron deflection (ξ) is 20 °= 0.349rad

The increment of the wing load due to the control deflection (L_{WO}) was calculated according to the method stated by Denis Howe and added to the wing-body load of the symmetric loading at trimmed steady level flight as detailed below:

$$L_{WO} = \rho V_o{}^2 S a_{2A}\xi/2 \tag{19}$$

where aileron lift curve slope, $a_{2a} = 3.42$/rad

Total wing-body load

$$Total\ L_{WB} = L_{WB} + L_{WO} \tag{20}$$

3.2. Load Distribution

Having obtained the design load on the wing, the next stage was to distribute the external forces in an appropriate way over the surface which generates them. These air-loads must be distributed in combination with the inertia distributions. Therefore, the span-wise lift distribution using the Schrenk's method [15,16] was established. An ideal semi-elliptical distribution, wing chord, and an average was plotted, see Fig 3.

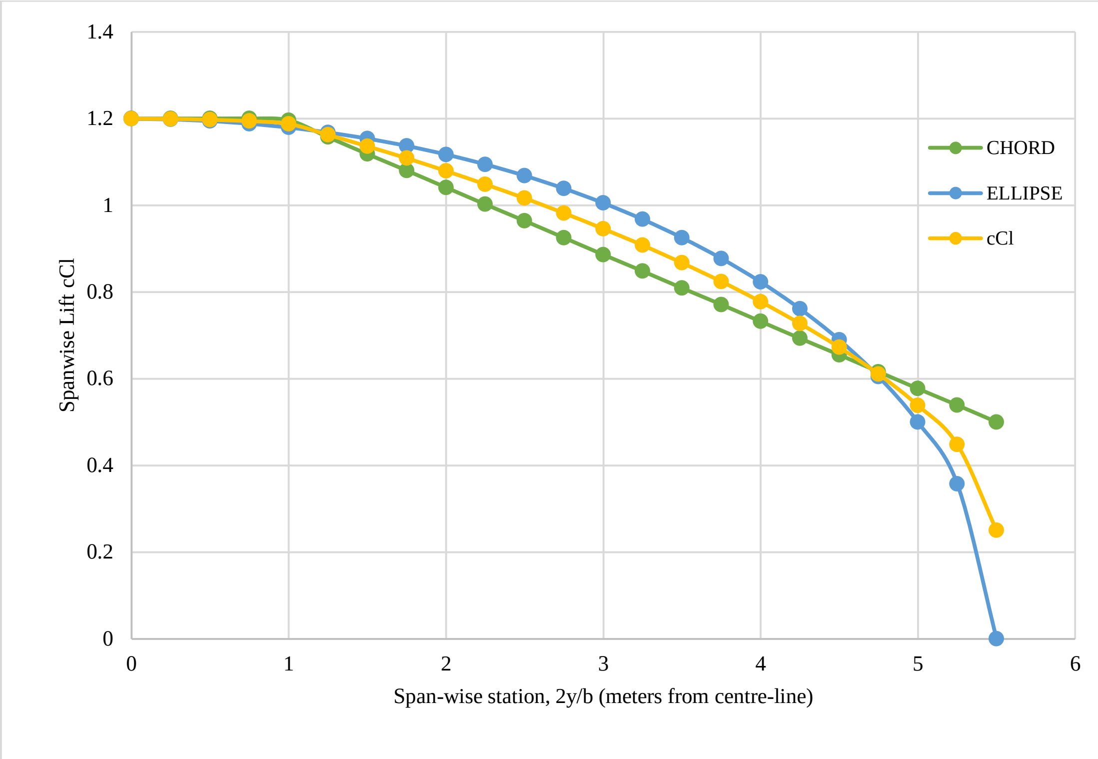

Fig. 3. Schrenk lift distribution

Since the wing is wetted with the incorporation of missile attachment as shown in Fig. 4, it was necessary to determine the inertia load due to the wing, fuel, and missile mass. The wing experiences shear and bending loads during maneuver or gust under the action of inertia and aerodynamic lift forces or air-load [13].

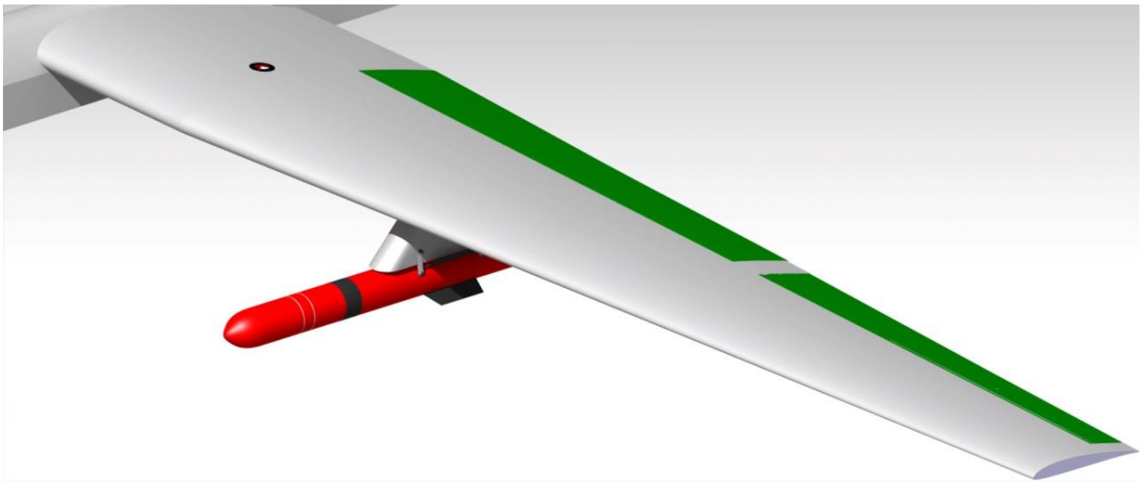

Fig. 4. CAD model of the wing assembly

Therefore, the next phase was to project its shear force and bending moment diagram as shown in Fig 5 and Fig 6 respectively. The calculations of the shear force and bending moment are given below for the 3.8g steady rotary case of the wing semi-span.

Having gotten the limit wing load, we derived the ultimate wing load as

$$L_w = 1.5 * L \tag{21}$$

where 1.5 is a factor of safety as specified in STANAG [10]. The shear force is obtained by integrating the distributed load over the semi-span of the wing using Equation (22).

$$SF_{lift(inertia)} = \int_0^{\frac{b}{2}} L_{W(inertia)}\, dy \tag{22}$$

where L_W is the aerodynamic lift acting on the entire wing has given in Equation (21). The maximum value for the total shear force was gotten as 12,555.28N.

The bending moment due to lift or inertia forces was calculated by integrating the shear force due to lift or inertia loads over the semi-span of the wing using Equation (23).

$$BM_{lift(inertia)} = \int_0^{\frac{b}{2}} SF_{lift(inertia)}\, dy \tag{23}$$

The value of the total bending moment was gotten as 35,714.92Nm. Table 3 shows the result of the total shear force and bending moment.

Table 3. Shear force and bending moment calculations result

SF due to lift	SF due to inertia	Total SF	BM due to lift	BM due to inertia	Total BM
0	0	0	0	0	0
507.224	-29.065	478.159	126.806	-7.266	119.540
1052.038	-60.283	991.755	389.816	-22.337	367.479
1634.443	-93.656	1540.787	798.426	-45.751	752.675
2254.926	-129.210	2125.716	1362.158	-78.053	1284.104
2912.999	-166.918	2746.080	2090.407	-119.783	1970.625
3608.662	-206.781	3401.881	2992.573	-171.478	2821.095
4342.404	-248.825	4093.579	4078.174	-233.684	3844.490
5113.736	-293.023	4820.713	5356.608	-306.940	5049.668
5922.658	-339.375	5583.283	6837.272	-391.784	6445.488
6769.170	-387.881	6381.289	8529.565	-488.754	8040.811
7653.273	-438.542	7214.732	10442.883	-598.390	9844.494
8575.454	-491.384	8084.071	12586.747	-721.236	11865.511
9535.226	-546.380	8988.846	14970.553	-857.830	14112.723
10532.587	-3398.425	7134.162	17603.700	-1707.437	15896.263
11568.027	-3457.757	8110.270	20495.707	-2571.876	17923.831
12641.057	-4107.907	8533.150	23655.971	-3598.853	20057.118
13751.678	-4780.833	8970.845	27093.890	-4794.061	22299.829
14900.377	-5476.831	9423.546	30818.984	-6163.269	24655.716
16070.067	-6185.547	9884.520	34836.501	-7709.655	27126.846
17241.711	-6895.447	10346.263	39146.929	-9433.517	29713.412
18413.354	-6962.584	11450.770	43750.268	-11174.163	32576.104
19584.998	-7029.721	12555.277	48646.517	-12931.593	35714.924

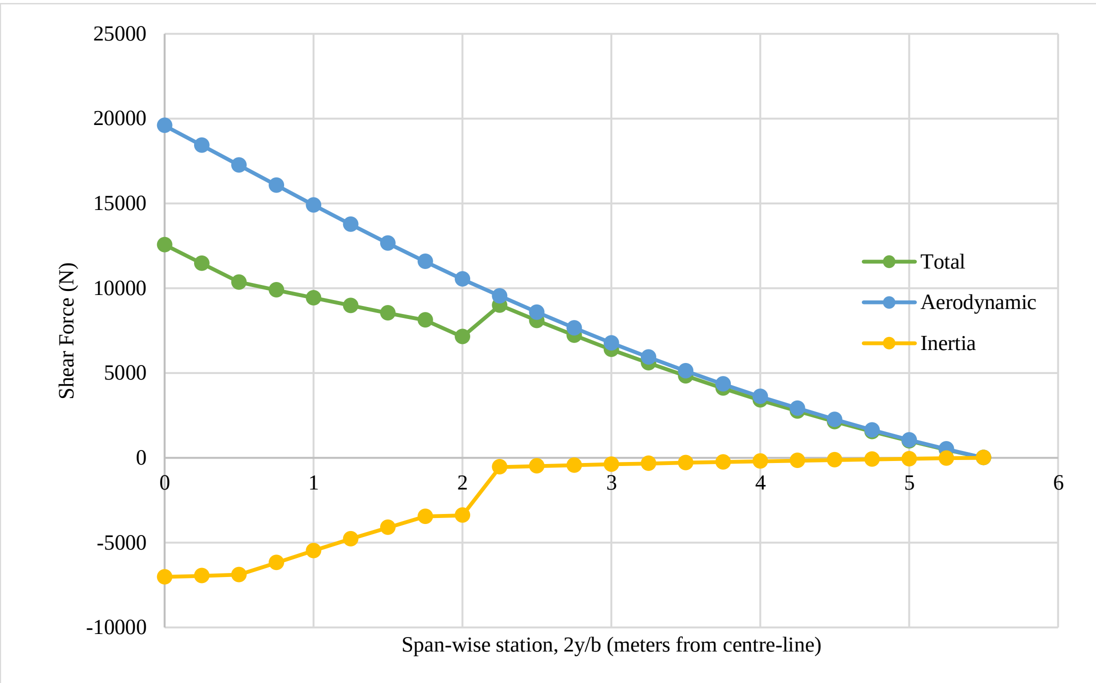

Fig. 5. Shear force diagram

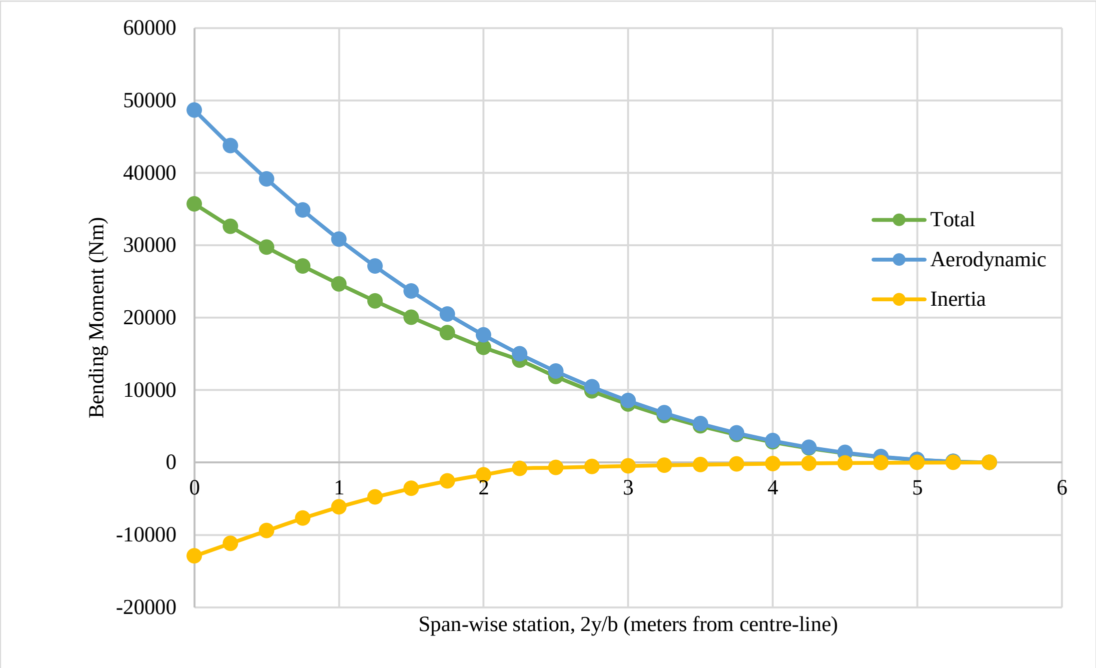

Fig. 6. Bending moment diagram

4. CAD Layout

The detailed design of the wing as shown in Fig. 7 reflects design modifications resulting from verification and validation of the finite element analysis. The CAD model of the entire wing assembly was designed using CATIA V5. The design approach emphasized structural simplification and reduced parts to minimize cost. The assembly drawing of the wing is shown in Fig. 4 which represents the final CAD model of the wing structure.

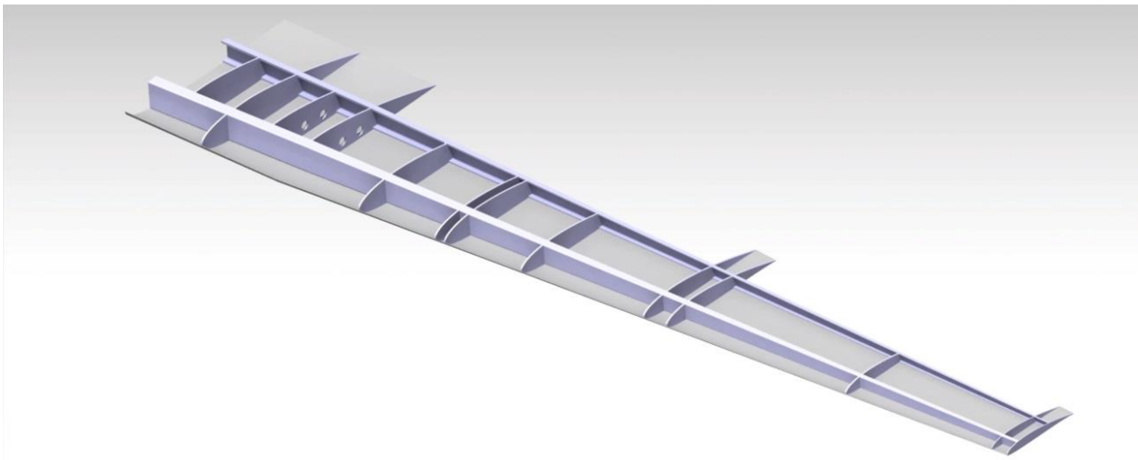

Fig. 7. Wing design showing the internal members

5. Results

Having derived the shear force and bending moment results, the Strand7 Finite Element Analysis Software was used to validate the results. The result of the analysis for the shear force and bending moment for the 3.8g steady rotary was obtained as shown in Fig. 8.

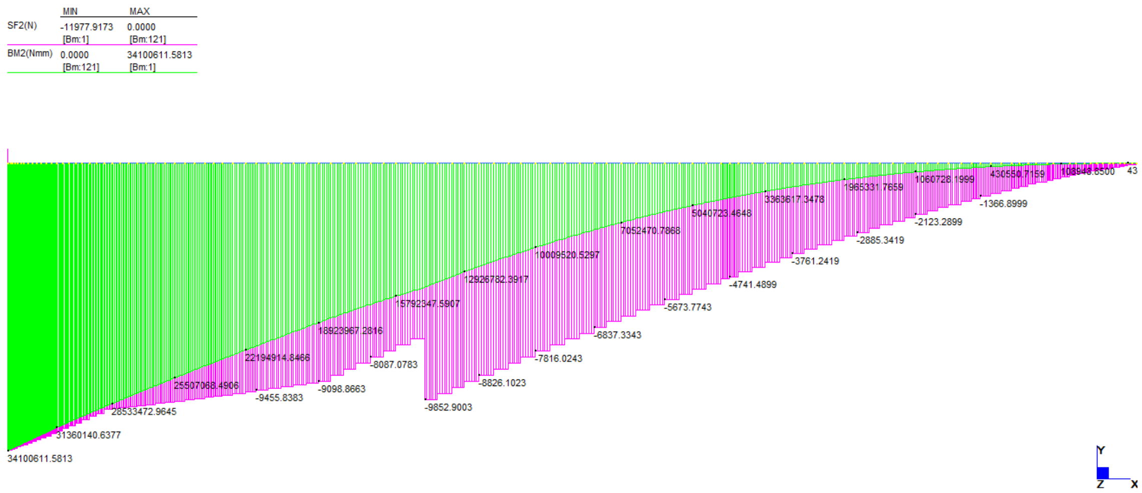

Fig. 8. 3.8g steady rotary shear force and bending moment diagram

Having derived the results from Strand7 software and Excel spreadsheet, the results were compared. Table 4 shows the comparison of the results.

Table 4. Comparison of results

	Maximum Shear Force			Maximum Bending Moment		
Load case	Excel (N)	Strand7 (N)	Error (%)	Excel (Nm)	Strand7 (Nm)	Error (%)
Steady rotary	12,555.28	11,977.92	4.82	35,714.92	34,100.61	4.73

6. Conclusion

At the initial design phase, a design environment for the lifting surfaces was created using the Athena Vortex Lattice software. Thereafter, the critical design case was established as the maximum aileron deflection at maximum take-off weight and maneuvering speed with a wing-body load of 27,488N. Furthermore, the maximum shear force and bending moment were derived as 12,555N and 35,715Nm respectively. Finally, the mass estimation for the proposed all composite structure was done using CATIA which weighed 56.64kg.

Acknowledgement

The successful completion of this project is strongly attributed to the entire staff and management of the Air Force Institute of Technology and the Nigerian Air Force.

References

[1] D. Howe, Aircraft Conceptual Design Synthesis, Suffolk: Professional Engineering Publishing Ltd, 2010.
[2] M. H. Sadraey, Aircraft Design: A Systems Engineering Approach, New Hampshire: John Wiley & Sons, Ltd, 2013.
[3] W. Grodzki and A. Łukaszewicz, "Design and manufacture of umanned aerial vehicles (UAV) wing structure using composite materials," Materials Science & Engineering Technology, vol. 46, no. 3, pp. 269-278, 2015.
[4] Airbus S.A.S., "Wing of the future - Company - Airbus," 17 January 2017. [Online]. Available: https://www.airbus.com/newsroom/news/en/2017/01/Wings-of-the-future.html. [Accessed 11 May 2019].
[5] R. E. Weibel and R. J. Hansman, "Safety Considerations for Operation of Different Classes of UAVs in the NAS," in AIAA 3rd "Unmanned Unlimited" Technical Conference, Workshop and Exhibit, Chicago, 2004.
[6] D. P. Raymer, Aircraft Design: A Conceptual Approach, Washington: American Institute of Aeronautics and Astronautics, Incorporated, 2018.
[7] T. L. Lomax, Structural Loads Analysis for Commercial Transport Aircraft: Theory and Practice, Reston: American Institute of Aeronautics and Astronautics, Incorporated, 1996.
[8] S. Gudmundsson, General Aviation Aircraft Design: Applied Methods and Procedures, Waltham: Elsevier Science, 2014.
[9] North Atlantic Treaty Organization, Standardization Agreement (STANAG) 4671, 2009.
[10] P. O. Jemitola and G. E. Abbe, Project Specification, Kaduna: Air Force Institute of Technology, 2018.
[11] D. Howe, Aircraft Loading and Structural Layout, Suffolk: Professional Engineering Publishing, 2004.
[12] J. R. Wright and J. E. Cooper, Introduction to Aircraft Aeroelasticity and Loads, West Sussex: John Wiley & Sons, Ltd, 2015.
[13] M. V. Cook, Flight Dynamic Principles, Burlington: Elsevier Ltd, 2007.
[14] O. Schrenk, "A simple approximation method for obtaining the span-wise lift distribution," in NACA Technical Memo No. 948, 1940.

[15] K. kundy, M. A. Prince and D. Riordan, Conceptual Aircraft Design: An Industrial Approach, West Sussex: John Wiley & Sons, 2019.
[16] M. Drela and H. Youngren, "Athena Vortex Lattice Program Version 3.36," Massachusetts Institute of Technology, Cambridge, 2016.
[17] J. W. Yu, "Design and Optimization of Wing Structure for a Fixed-Wing Unmanned Aerial Vehicle (UAV)," Modern Mechanical Engineering, vol. 8, pp. 249-263, 2018.
[18] Y. Naidu and S. Adali, "Design and Optimization of a Medium Altitude Long Endurance UAV Wingbox Structure," R & D Journal of the South African Institution of Mechanical Engineering, vol. 30, pp. 22-29, 2014.
[19] H. R. Chauhan, H. Panwar and V. Rastogi, "Structural Design & Optimization of an Unmanned Aerial Vehicle Wing for SAE Aero Design Challenge," International Journal of Advance Research and Innovation, vol. 5, no. 1, pp. 24-29, 2017.

Authors' Profiles

Oluwafemi Anthony Adeleke (born February 5, 1994) is a student at Air Force Institute of Technology (AFIT), Kaduna and a Functional Consultant at Ramco Systems Limited.

Godwin Esosa Abbe (PhD) is the Air Assistant to the Commandant, Armed Forces Command and Staff College (AFCSC), Jaji, Kaduna. He is also a Senior Lecturer at the Faculty of Air Engineering, AFIT, Kaduna.

Paul Olugbeji Jemitola (PhD) is the Principal Director, Air Force Research and Development Center (AFRDC), Kaduna. He is also a Senior Lecturer in AFIT and a senior engineer at Vector Aeronautics

Thomas Sadiq (Assoc. Prof.) is the Head of Department, Computer Engineering Department at Nile University of Nigeria Abuja. He was a senior lecturer at the Department of Aerospace Engineering, AFIT, Kaduna.

How to cite this paper: Oluwafemi A. Adeleke, Godwin E. Abbe, Paul O. Jemitola, Sadiq Thomas, " Design of the Wing of a Medium Altitude Long Endurance UAV ", International Journal of Engineering and Manufacturing (IJEM), Vol.12, No.1, pp. 37-47, 2022. DOI: 10.5815/ijem.2022.01.04